論文 한국공작기계학회지 제 8 권 제 1 호 1999. 2.
Journal of the Korean Society of Machine Tool Engineers

PREVIEW CONTROL FOR EDGE-FOLLOWING USING ROBOT FORCE CONTROL

Boojoong Yong*

Abstract

This paper presents a discrete-time model of an edge-following with accommodation force control. Since an irregular workpiece shape causes disturbances to the system while following an edge, the use of preview control is proposed to improve the system performance. The preview control employs future information of the workpiece contour shape, and it can be developed by LQ-optimal control principles. This study provides a general method how to utilize the local future information obtained by the finite preview to minimize an optimality criterion evaluated over a problem duration. The force controller is designed based on the preview control scheme, and then implemented on a VME-based computer. Experimental results using an industrial robot show that the preview control system achieves faster tracking speed and better force regulation than the conventional nonpreview control system.

Keywords : Edge-Following, Accommodation Control, Preview Control, FEP (Force Control Enhanced By Preview Control), FDP (Force Controller Designed By Preview Control Algorithm)

1. INTRODUCTION

When a robot manipulator interacts mechanically with its environment to perform tasks such as assembly or edge-finishing, the end-effector is thereby constrained by the environment. Robot force control is necessary, since it increases safety due to monitoring of contact force. A comparison of various force control architecture is reported[12]. Different force control methods can often be configured to achieve similar results for a given task, and the choice of control algorithm depends strongly on the application or on the characteristics of a particular robot. Accommodation control is one of the early force control approaches[11]. Because of the relationship between force and velocity, accommodation may also be called damping control. Edge-following is controlling a robot manipulator to follow along an unknown irregularly shaped workpiece surface while maintaining a desired contact force [6, 8]. The edge-following can be applied to deburring to

* Kyungil University Department of Mechanical Engineering

avoid complexity of programming the robot motion, to reduce teaching time, and to improve quality of products[3]. Shape recovery is also useful application of the edg-following for self-teaching robots and for exploratory operations in unknown environments[1].

In designing a control system, it is usually assumed that the future is unknown and is unpredictable. A consequence of this assumption is that the feedback structure of a control system is decided upon by operating on an instantaneous error. If information about the reference input or the disturbance is known a priori, it is reasonable to expect some performance improvements over conventional feedback control. Preview control exploits this idea with the aid of LQ-optimal control theory[9, 10]. This paper extends the properties of the optimal servo problem [4] to the preview concept, which is well suited for the edge-following. For good tracking behavior and good force regulation, the preview controller anticipates incremental changes for subsequent interactions.

In this study, a discrete-time model of the edge-following is proposed according to the accommodation force control, and the use of optimal preview control is given. For designing adequate force controllers, two design approaches via preview control are presented. To test their effectiveness, the designed force controllers are implemented on a VME-based computer, and the performance improvements are evaluated using a PUMA 560 industrial robot. Experimental results of the edge-following under the influence of preview control are reported, where performance is measured in terms of rms force error for force regulation and tangential tracking speed for robustness.

2. SYSTEM MODELING

2.1 Edge-following algorithm

Considering realistic automation tasks, the complete procedure of force controlled edge-following may be described by the following three modes: (1) approach phase and transition mode, (2) edge-following, and (3) termination. Approa-ching a workpiece with a priori unknown position, the robot manipulator collides with the workpiece eventually, and a conditional stop occurs upon a detection of the predetermined contact force level. Edge-following mode is activated after establishing a bias force in the normal direction of the contour. The robot manipulator follows along the workpiece edge with a prescribed tangential velocity maintaining the constant bias force. The actual contact force is fed back and used to generate compensatory motions which remove the normal contact force error. Finally, the edge-following mode terminates if any termination condition occurs, e.g., an excessive force threshold or a saturation of actuators, elapse of execution time, intolerable disturbance, or any combination of such conditions.

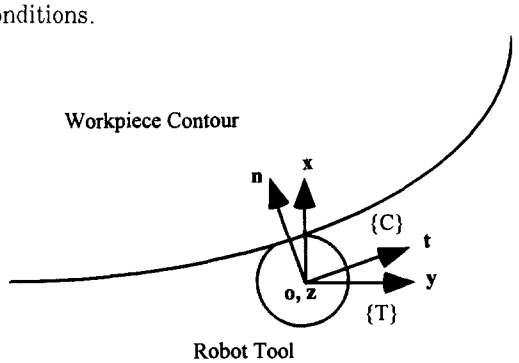

Fig. 1 Tool-Workpiece coordinates

In order to realize the edge-following system, two coordinate frames are introduced: {C} the workpiece contour constraint frame and {T} the robot tool frame. As shown in Fig. 1, the constraint frame is defined by the normal **(n)** and tangential **(t)** direction of the contour, while the robot tool frame is located at the center of

the tool with principal axes **x**, **y**, and **z**. The constraint frame moves along the workpiece edge tangential direction. In this work, the orientation of the tool coordinate frame is maintained constant with respect to the robot world coordinate, thus the normal direction to the contour must be force controlled and the tangential direction of this contour must be position or velocity controlled. Coordinate trans -formations which relate these two coordinates will be obtained from the measured feedback force information, and will be automatically updated in the force control law.

2.2 Edge-following loop closure

In this investigation, the robot manipulator has provision for user-modification of velocity, and thus the edge-following uses an accommodation force control. The complete edge-following system is represented by the block diagram of Fig. 2.

Note that this system contains an integrator, since it is constructed based on accommodation control. $\frac{T}{2}\frac{z+1}{z-1}$ is a Z-transform of an integrator

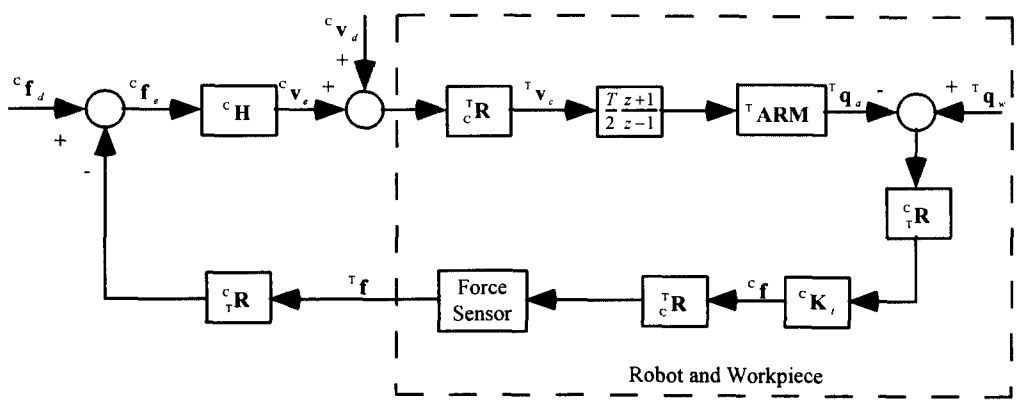

Fig. 2 Edge-following using accommodation

$^{c}\mathbf{f}_d$: desired contact force
$^{c}\mathbf{f}_e$: force error
$^{c}\mathbf{f}$: actual contact force
$^{T}\mathbf{f}$: measured force
$^{c}\mathbf{v}_e$: velocity error
$^{c}\mathbf{v}_d$: desired tangential velocity
$^{T}\mathbf{v}_c$: velocity command
$^{T}_{c}\mathbf{R}, ^{c}_{T}\mathbf{R}$: coordinate transformation matrices
$^{c}\mathbf{H}$: force controller matrix
$^{c}\mathbf{K}_t$: total system stiffness matrix
$^{T}\mathbf{q}_w$: workpiece position
$^{T}\mathbf{q}_a$: actual manipulator tool position
$^{T}\mathbf{ARM}$: robot closed-loop Cartesian position dynamics in translational motion

$$^{c}\mathbf{f}_d=\begin{bmatrix} f_d(k) \\ 0 \end{bmatrix},\ ^{c}\mathbf{f}=\begin{bmatrix} f(k) \\ 0 \end{bmatrix},\ ^{c}\mathbf{v}_d=\begin{bmatrix} 0 \\ v_d(k) \end{bmatrix},\ ^{T}\mathbf{f}=\begin{bmatrix} f_x(k) \\ f_y(k) \end{bmatrix},\ ^{c}\mathbf{H}=\begin{bmatrix} H(z) & 0 \\ 0 & 0 \end{bmatrix},\ ^{c}\mathbf{K}_t=\begin{bmatrix} K_t & 0 \\ 0 & 0 \end{bmatrix},\ ^{T}\mathbf{q}=\begin{bmatrix} q_x(k) \\ q_y(k) \end{bmatrix},$$

$$^{T}_{c}\mathbf{R}=[\mathbf{n}\quad \mathbf{t}],\ \mathbf{n}=\frac{1}{\|^{T}\mathbf{f}\|}\begin{bmatrix} f_x(k) \\ f_y(k) \end{bmatrix},\ \mathbf{t}=\frac{1}{\|^{T}\mathbf{f}\|}\begin{bmatrix} -f_y(k) \\ f_x(k) \end{bmatrix},\ \mathbf{n}\bullet\mathbf{t}=0,\ ^{T}\mathbf{ARM}=\begin{bmatrix} G_x(z) & 0 \\ 0 & G_y(z) \end{bmatrix}$$

according to Tustin's bilinear rule, where T represents a 28ms of sampling period, and z represents the Z-transform variable. ${}^{C}(\cdot)$ denotes the contour constraint frame relativity, ${}^{T}(\cdot)$ the tool frame relativity, and $\|\cdot\|$ the Euclidean norm. The velocity error ${}^{C}\mathbf{v}_e$ in the normal direction and the desired tangential velocity ${}^{C}\mathbf{v}_d$ are transformed into a velocity command ${}^{T}\mathbf{v}_c$ via transformation matrix ${}^{T}_{C}\mathbf{R}$. In the robot tool frame, the velocity commands in x and y axes drive the robot manipulator. ${}^{T}\mathbf{ARM}$ consists of the Cartesian closed-loop positional robot dynamics along x and y directions, assuming the dynamics of all translational motions are dynamically decoupled and identical. This assumption is valid if the robot system is engaged in the task with slow dynamic motions, e.g., controlling fine motions of the robot, and results in $G(z)=G_x(z)=G_y(z)$. Experimental system identification also verifies the assumption. The interaction between the manipulator and the workpiece causes the normal contact force through their combined mechanical impedance. Here, only the stiffness component of that impedance is considered, since low bandwidth (i.e., slow motion) is expected in this work. The force error formed in {C} is processed by the accommodation force control, ${}^{C}\mathbf{H}(z)$.

3. PREVIEW CONTROL SCHEME

The proposed control method requires a linearized plant model to design the control law. In this section, a linear discrete-time model for the edge-following is introduced, and then based on this model, the optimal preview control law is presented.

The linear plant model can be represented by the discrete-time state-space equations such as

$$\begin{aligned}\mathbf{x}(k+1) &= \Phi\mathbf{x}(k)+\Gamma u(k)\\ y(k) &= \mathbf{H}\mathbf{x}(k)\end{aligned} \tag{1}$$

where Φ is an $n\times n$ system matrix, Γ is an n-dimensional column vector, H is an n-dimensional row vector, $\mathbf{x}(k)$ is an n-dimensional state vector, and u(k), y(k) are control input and system output, respectively. In order to improve the performance of the edge-following, the geometry of the workpiece contour can be used for preview information. The workpiece position may be sensed by a robot-mounted sensor traveling some distance ahead of the robot manipulator or may be available from a database obtained independently. Then the anticipated force error due to workpiece position disturbance in {C} can be deduced by [13]

$$\begin{aligned}\mathbf{x}_p(k+i) &= {}^{C}\mathbf{K}_t\,{}^{C}_{T}\mathbf{R}\,{}^{T}\mathbf{q}_w(k+i)\\ &= \begin{bmatrix} x_p(k+i)\\ 0\end{bmatrix} \qquad ;\ i=1,\ldots,N_p\end{aligned} \tag{2}$$

where ${}^{T}\mathbf{q}_w(k+i)$ is a workpiece position measured i-th step ahead in the robot tool frame {T}, and N_p the finite preview length. The preview servo dynamics are then [7]

$$\begin{aligned}\mathbf{x}_p(k+1) &= \tilde{\Phi}\mathbf{x}_p(k)\\ x_p(k) &= \tilde{\mathbf{H}}\mathbf{x}_p(k)\end{aligned} \tag{3}$$

where $\tilde{\Phi}$ is an $(N_p+1)\times(N_p+1)$ matrix, $\mathbf{x}_p(k)$ is an (N_p+1)-dimensional preview state vector, $\tilde{\mathbf{H}}$ is an (N_p+1)-dimensional row vector, and

$$\mathbf{x}_p(k)=\left[x_p(k)\quad x_p(k+1)\quad x_p(k+2)\quad \cdots\quad x_p(k+N_p)\right]^{\mathrm{T}}$$

$$\tilde{\mathbf{H}}=\begin{bmatrix}1 & 0 & \cdots & 0\end{bmatrix}$$

$$\tilde{\Phi}=\begin{bmatrix}0 & 1 & 0 & \cdots & . & 0\\ 0 & 0 & 1 & \cdots & . & 0\\ . & . & . & \cdots & . & .\\ . & . & . & \cdots & . & .\\ . & . & . & \cdots & 0 & 1\\ 0 & . & . & \cdots & -1 & 2\end{bmatrix} \tag{4}$$

The linear plant model (1) is augmented by adding the preview servo dynamics (3), and the augmented system can be represented as

$$\begin{aligned}\mathbf{z}(k+1)&=\mathbf{A}\mathbf{z}(k)+\mathbf{B}u(k)\\ e(k)&=\mathbf{C}\mathbf{z}(k)\end{aligned} \tag{5}$$

where

$$\mathbf{A}=\begin{bmatrix}\Phi & \mathbf{0}\\ \mathbf{0} & \tilde{\Phi}\end{bmatrix},\quad \mathbf{B}=\begin{bmatrix}\Gamma\\ \mathbf{0}\end{bmatrix},\quad \mathbf{C}=\begin{bmatrix}\mathbf{H} & -\tilde{\mathbf{H}}\end{bmatrix},$$

$$\mathbf{z}(k)=\begin{bmatrix}\mathbf{x}(k)\\ \mathbf{x}_p(k)\end{bmatrix} \tag{6}$$

and e(k) represents a force error.

The proposed control system applies optimal preview control to the augmented system. The resulting control law can be expressed by [13]

$$u(k)=-\mathbf{K}\mathbf{x}(k)-\mathbf{K}_p\bar{\mathbf{x}}_p(k) \tag{7}$$

where

$$\mathbf{K}=\left\{\Gamma^{\mathrm{T}}\mathbf{S}_{11}\Gamma+R\right\}^{-1}\Gamma^{\mathrm{T}}\mathbf{S}_{11}\Phi \tag{8}$$

$$\begin{aligned}\mathbf{K}_{ff}&=\left\{\Gamma^{\mathrm{T}}\mathbf{S}_{11}\Gamma+R\right\}^{-1}\Gamma^{\mathrm{T}}\mathbf{S}_{12}\tilde{\Phi}\\ &=\begin{bmatrix}0 & \mathbf{K}_p\end{bmatrix}\end{aligned} \tag{9}$$

$$\mathbf{S}=\mathbf{A}^{\mathrm{T}}\mathbf{S}\mathbf{A}-\mathbf{A}^{\mathrm{T}}\mathbf{S}\mathbf{B}\left\{\mathbf{B}^{\mathrm{T}}\mathbf{S}\mathbf{B}+R\right\}^{-1}\mathbf{B}^{\mathrm{T}}\mathbf{S}\mathbf{A}+\mathbf{C}^{\mathrm{T}}Q\mathbf{C} \tag{10}$$

$$\mathbf{S}=\begin{bmatrix}\mathbf{S}_{11} & \mathbf{S}_{12}\\ \mathbf{S}_{21} & \mathbf{S}_{22}\end{bmatrix},\quad \mathbf{S}_{21}=\mathbf{S}_{12}^{\mathrm{T}} \tag{11}$$

$$\bar{\mathbf{x}}_p(k)=\left[x_p(k+1)\quad x_p(k+2)\quad \cdots\quad x_p(k+N_p)\right]^{\mathrm{T}} \tag{12}$$

and R and Q are positive scalar weighting functions.

The control law (7) consists of a feedback controller and a feedforward controller. The optimal feedback controller, $\mathbf{K}$ (n-dimensional gain vector), ensures a good system dynamic performance as well as a closed-loop system stability. The feedforward preview controller, $\mathbf{K}_p$, is an N_p-dimensional gain vector which addresses force errors induced by workpiece position disturbances. If no preview information is available, the control law results in a conventional LQ-optimal controller. Note that the augmented system (5) is uncontrollable since there is no feedback loop to the preview servo mechanism. However, the control law, u(k), exists and the resulting closed-loop system is asymptotically stable if the system (Φ,Γ) is completely controllable. It is also shown that the preview gain vector, $\mathbf{K}_p$ exists if the product of any eigenvalue of $\tilde{\Phi}$ and any eigenvalue of the closed-loop system lies within a unit circle at the origin of the complex plane [13]. Once the feedback controller is designed, the preview gain vector can be determined based on the feedback control gains.

Since the full system state, $\mathbf{x}(k)$, is not directly accessible, a state estimator is required in the feedback loop. Force measurements from a wrist force sensor include measurement noise, and the robot system contains unmodeled dynamics and unknown disturbances. Optimal estimation method combines the information from the noisy measurements with the information implicit in the estimator model equation [5]. For this reason, we choose an optimal state estimator which handles noise contaminated systems effectively. If we feed back the force error, e(k), we can obtain the estimated state vector $\hat{\mathbf{x}}(k)$ such as

$$\hat{\mathbf{x}}(k) = \bar{\mathbf{x}}(k) + \mathbf{L}\{e(k) - \mathbf{H}\bar{\mathbf{x}}(k)\} \tag{13}$$

where $\mathbf{L}$ is the constant Kalman gain, and $\bar{\mathbf{x}}(k)$ is the time updated state from

$$\bar{\mathbf{x}}(k+1) = \Phi\hat{\mathbf{x}}(k) + \Gamma u(k) \tag{14}$$

Fig. 3 shows the edge-following system using the preview controller and the Kalman filter. In Fig. 3, the external reference input, r(k), represents a desired contact force, and y(k) an actual contact force. The feedback portion consists of the optimal state estimator and the optimal controller, while the feedforward portion is a weighted sum of force errors by preview.

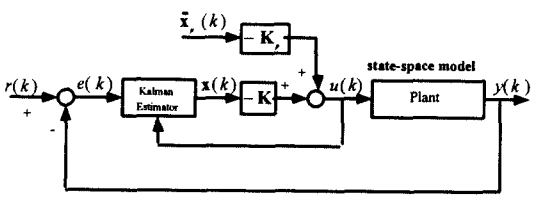

Fig. 3 Edge-following system with optimal preview control

4. FORCE CONTROL LAW FOR EDGE-FOLLOWING

The contour-following system involves force control as well as velocity control. The constant tangential velocity is directly fed to the robot positioning system, while the force controller regulates force error regarding normal direction to the contour. Assuming linearity, after designing a force controller, the constant tangential velocity can be introduced to complete the contour-following system. Now, it is necessary to obtain the dynamic model of the robot manipulator for designing the force control law. The modeling of robot dynamics is quite complex and requires physical data which is often unavailable. In this investigation, the robot's arm dynamics are obtained by a system identification procedure using experimental data. Although the real robot system is fully nonlinear, the identified linear model (15) is well suited for the problem analysis, and is useful for designing and testing control strategies:

$$G(z) = 0.003343\frac{z^{-1} + 20.6890z^{-2} + 157.1410z^{-3}}{1 - 0.2810z^{-1} - 0.0349z^{-2} - 0.0863z^{-3}} \tag{15}$$

In Section 4.1, the force controller is designed using a root locus method, which results in a conventional linear controller. In Section 4.2, considering analytic features of the preview control, two design approaches are proposed: FEP (Force Control Enhanced by Preview Control) and FDP (Force Controller Designed by Preview Control Algorithm)

4.1 Conventional linear control

From Fig. 2 and block-diagram analysis, the characteristic equation of the force control loop in the normal direction of the contour is derived by

$$1 + \frac{T}{2}\frac{z+1}{z-1}K_t H(z)G(z) = 0 \tag{16}$$

where the total system stiffness (robot arm and workpiece), K_t, is measured to be 13,850 N/m. For design criteria, the dynamic characteristics (rise time, overshoot, settling time, bandwidth, etc.) of the arm dynamics are considered to achieve the desired force response. The lead compensator is determined as

$$H(z) = 2.058 \times 10^{-3}\frac{z - 0.5890}{z + 0.5650} \tag{17}$$

This force controller yields the transient mode of

the force control loop having almost the same dynamic behavior as the inner position control loop.

4.2 Force control using preview control

FEP enhances the dynamic performance of the standard force-controlled edge-following using a preview controller. The main purpose of FEP is to obtain a better performance without modifying a pre-existing control system. Thus FEP provides a portability, and does not alter any existing controller or the system. In this case, the plant in Fig. 3 consists of forward path of the edge-following system including the designed linear force controller (see Fig. 2). On the other hand, FDP allows a force controller directly designed by the preview control technique. Therefore, in FDP, the plant to be controlled is simply composed of robot and workpiece dynamics, and the preview controller becomes a part of the force controller.

The use of optimal preview control is often hampered by the conflict between mathematical analysis and practical implementation. The design of control law stems from the choice of weighting function ratio, $\rho_c = Q/R$, for single -input single-output system. The weighting function ratio addresses the dynamic behavior of the closed-loop system and must be chosen carefully. The larger the ratio, the larger will be the elements of feedback gain. The speed of the controlled system is slow with a low value of ρ_c. The magnitude of the elements of $\mathbf{K}$ and $\mathbf{K}_f$ should be limited by actual system components, and thus ρ_c should often be adjusted by an iterative process. Selection of ρ_c is not straight forward nor unique, and is a trade-off to meet the required performance specifications, such as smooth tracking with robustness and an appropriate magnitude of control input. In this study, the weighting function ratio is found to be $\rho_c = 45.7$ for FEP and $\rho_c = 17,370$ for FDP, respectively. Among several preview lengths tested for experiments, the 5-step preview yielded the best results. Adequate optimal state estimators are also experimentally found by the iterative method so that the Kalman filter removes the undesired oscillation without introducing too much lag and slowing the response. The system models and the designed gains ($\mathbf{K}$, $\mathbf{K}_f$, L) are given in Appendix A.

5. EXPERIMENTAL RESULTS

5.1 Experimental system

The experimental apparatus includes a Sun SPARC station 330 (host computer), a VME computer (target computer), a PUMA 560 robot manipulator with a standard Unimation controller, an Astek FS6-120A 6-axis wrist force sensor. Overall system layout is shown in Fig. 4.

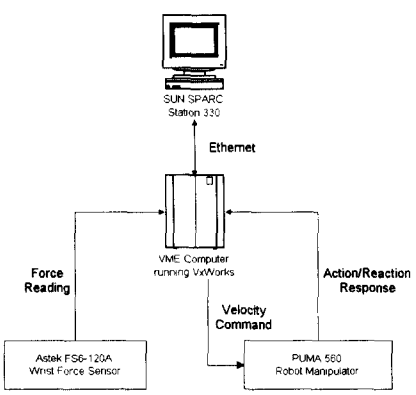

Fig. 4 Schematic diagram of hardware

Control software is programmed on the host computer (UNIX-based SunOS), and then

downloaded to the target computer running VxWorks, a real-time operating system. The VME computer incorporates the robot's motions and feedback/feedforward information. The standard Unimation controller with VAL-II robot programming language allows the external VME computer to modify the robot's motion in a real-time at a rate of 35Hz.

The edge-following systems (standard system, FEP, and FDP) are tested on three separate tasks at tangential speed of 15, 20, and 23mm/sec. within a bias force range of 9.5N ~ 14.0N: (1) following a straight edge, (2) encountering a 30 ° step change in the contour, and (3) following a curved contour of 40mm radius of curvature. Performance is characterized in two ways: comparison of rms (root-mean -square) force error, and amount of increase in tangential tracking speed that may be tolerated while maintaining a desired force level. The second measure is an indication of the robustness of the system.

5.2 Following a straight edge

Figs. 5 ~ 7 show typical force response for straight edge-following with a 20mm/sec. of tangential tracking speed.

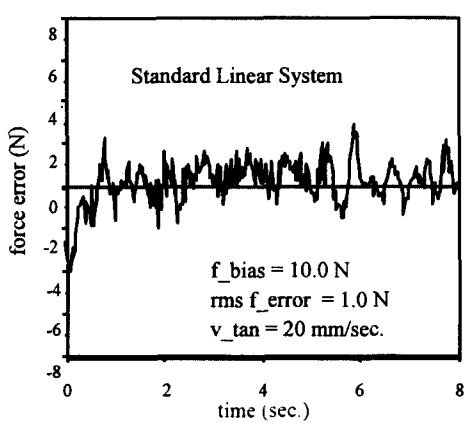

Fig. 5 Force error with a standard controller

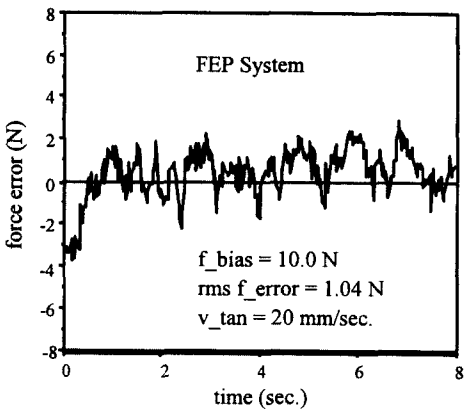

Fig. 6 Force error with FEP

The small amplitude limit cycle oscillations observed in the results may be due to the unmodeled high frequency dynamics or mechani cal vibrations. Fig. 8 presents that preview control does not really reduce the force error compared to nonpreview control system in this test. Indeed, this is not a surprising result, since we do not expect any notable advantage from a preview for the straight edge. These results imply that the preview control may not be necessary at low tracking speeds or for workpieces which do not contain any curvature. However, maximum tangential tracking speed is improved from 62mm/sec. (for standard system) to 72mm/sec by FEP and 93mm/sec. by FDP, respectively.

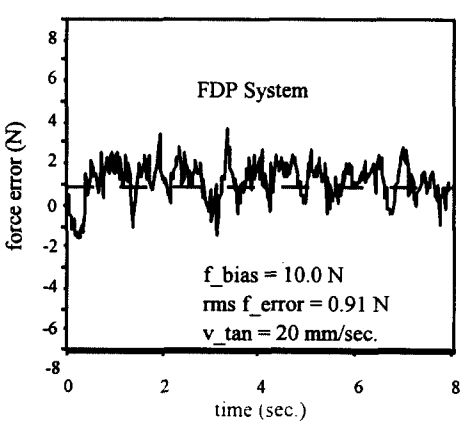

Fig. 7 Force error with FDP

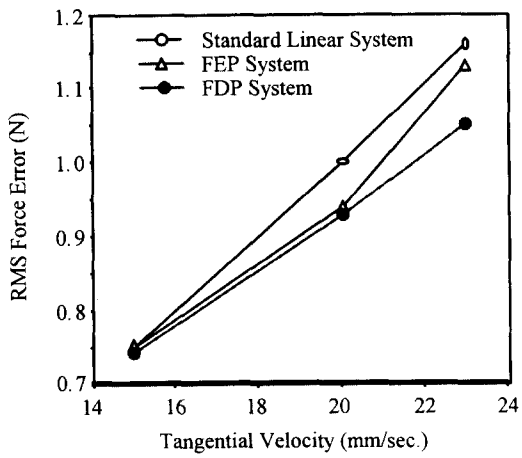

Fig. 8 RMS force error with respect to tangential velocity

5.3 Encountering a step change in contour

The workpiece edge with a 30 ° slope is shown in Fig. 9, and the system behavior maintaining the tangential speed of 20mm/sec. is illustrated in Figs. 10 ~ 12. In this experiments, rms force error is not calculated since the major concern is to examine the disturbance rejection and the behavior of the system encountering a sharp corner.

Experiencing a step disturbance, the nonpre -view control system shows an extensive force error, meanwhile FEP and FDP achieve stable motion with much less peak force error. Observed maximum tolerable tracking speed is: 23mm/sec. by standard control, 28mm/sec. by FEP, and 32mm/sec. by FDP, respectively.

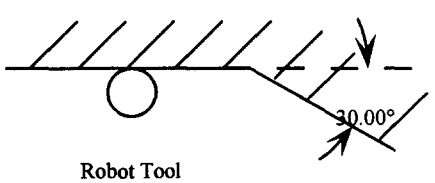

Fig. 9 Workpiece edge with a sharp corner

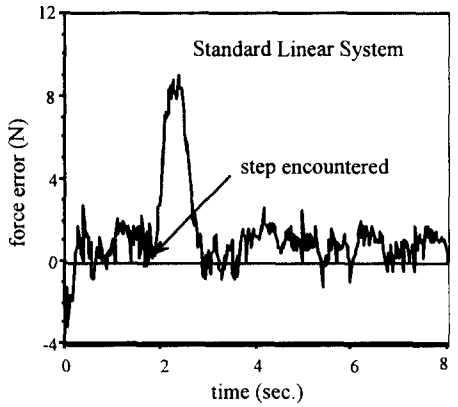

Fig.10 Force error with a standard controller

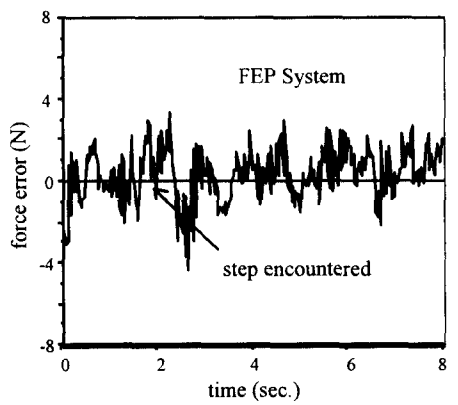

Fig. 11 Force error with FEP

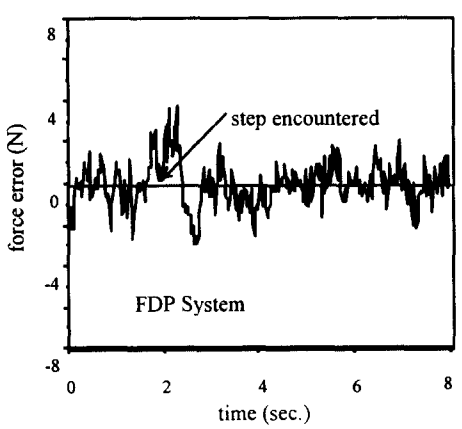

Fig. 12 Force error with FDP

5.4 Following a curved contour

Figs. 14 ~ 16 present force error profile during following a curved edge. The effect of preview is apparent in reducing sinusoidal workpiece position disturbance as shown in Fig. 13, and is more pronounced at higher tangential following speed (see Fig. 17).

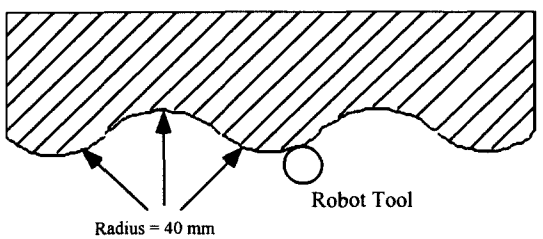

Fig. 13 Configuration of workpiece edge

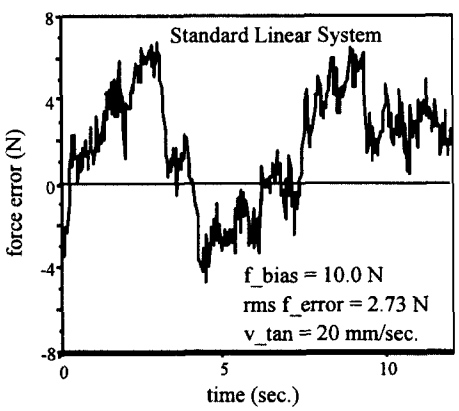

Fig. 14 Force error with a standard controller

Note that the rms force error with preview is similar to the results of the straight edge-following. Unlike the standard control system, the preview control systems are not significantly affected by a variation of tangential tracking speed. This implies the robustness of preview control. Acceptable highest tangential following speed is observed by 24mm/sec. for standard system, 29mm/sec. for FEP, and 32mm/sec. for FDP, respectively.

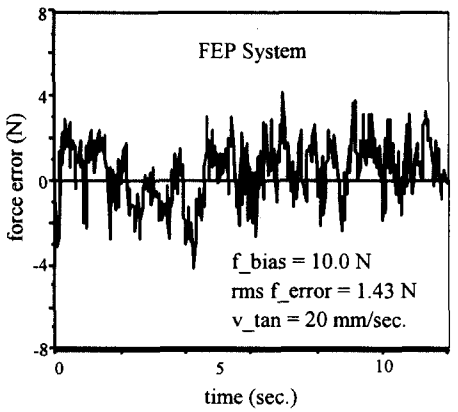

Fig. 15 Force error with FEP

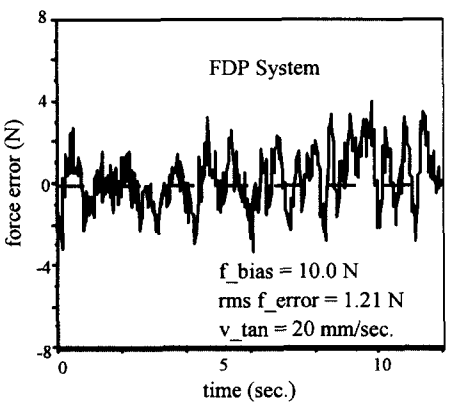

Fig. 16 Force error with FDP

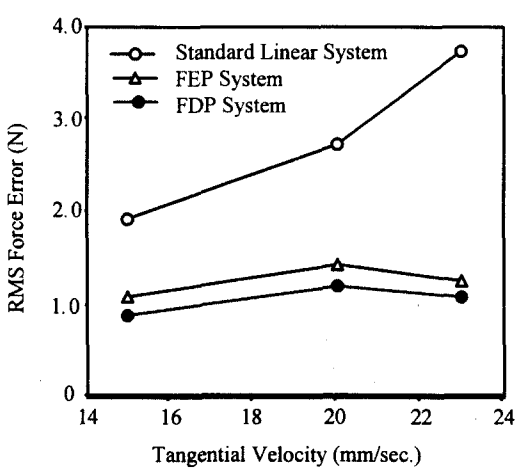

Fig. 17 RMS force error with respect to tangential velocity

6. CONCLUSION

An edge-following system is modeled using accommodation force control. Application of an optimal finite preview control to the edge-following is investigated, in an effort to reduce rms force error and to increase tangential tracking speed. A simple method for designing the preview control system is proposed. To verify the effectiveness of preview control, experiments are carried out using a PUMA 560 industrial robot.

Theoretically, longer preview will result in better performance, and there is no direct relationship between the preview length and the stability [9]. However, this study shows that there exists a maximum effective preview length which optimizes the system performance. For the specific robot force control employed here, the best performing preview distance is found experimentally. Experimental results reveal that the preview control is very useful for this type of force control, yielding much better force regulations and disturbance rejections over the nonpreview control.

REFERENCES

1. Ahmad, S., and Lee, C., "Shape Recovery From Robot Contour-Tracking With Force Feedback," Proc. IEEE Int. Conf. on Robotics and Automation, pp. 447-452, 1990.
2. Anderson, B., and Moore, J. B., Optimal Control: Linear Quadratic Methods, Prentice Hall, Inc., Englewood Cliffs, N.J., 1990.
3. Her, M. G., and Kazerooni, H., "Automated Robotic Deburring Of Parts Using Compliance Control," ASME Journal of Dynamic Systems, Measurement, and Control, Vol. 113, No. 1, pp. 60-66, March 1991.
4. Kreindler, E., "On the Linear Optimal Servo Problem," Int. Journal Of Control, Vol. 9, No. 4, pp. 465-472, Dec. 1969.
5. Lewis, F. L., Optimal Estimation, John Wiley & Sons, Inc., 1986.
6. Merlet, J-P, "C-Surface Applied To The Design Of An Hybrid Force-Position Robot Controller," Proc. IEEE Int. Conf. on Robotics and Automation, pp. 1055-1059, 1987.
7. Pak, H. A., and Turner, P. J., "Optimal Tracking Controller Design For Invariant Dynamics Direct-Drive Arms," ASME Journal of Dynamic Systems, Measurement, and Control, Vol. 108, No. 4, pp. 360-365, Dec. 1986.
8. Starr, G. P., "Edge-Following With A PUMA 560 Manipulator Using VAL-II," Proc. IEEE Int. Conf. on Robotics and Automation, pp. 379-384, 1986.
9. Tomizuka, M., and Whitney, D. E., "Optimal Discrete Finite Preview Problems (Why and How is future information important?)," ASME Journal of Dynamic Systems, Measurement, and Control, Vol. 97, No. 4, pp. 319-325, Dec. 1975.
10. Tomizuka, M., and Rosenthal, D. E., "On The Optimal Digital State Vector Feedback Controller With Integral And Preview Actions," ASME Journal of Dynamics Systems, Measurement, and Control, Vol. 101, No. 2, pp. 172-178, June 1979.
11. Whitney, D. E., "Force Feedback Control Of Manipulator Fine Motions," ASME Journal of Dynamic Systems, Measurement, and Control, Vol. 99, No. 2, pp. 91-97, June 1977.
12. Whitney, D. E., "Historical Perspective And State Of The Art In Robot Force Control," Int. Journal of Robotics Research, Vol. 6, No. 1, pp. 3-17, March 1987.
13. Yong, B., and Starr, G. P., "Preview Control For Edge-Following Of An Industrial Robot," Proc. of ASME International Mechanical Engineering Congress and Exposition, pp.

107-113, San Francisco, CA, Nov. 1995.

APPENDIX A

In the linear plant model Eq. (1), the followings represent FEP system and FDP system along with the resulting gains:

(1) FEP System

$$\Phi = \begin{bmatrix} 0.12699 & 1 & 0 & 0 \\ 0.55246 & 0 & 1 & 0 \\ 0.23776 & 0 & 0 & 1 \\ 0.08278 & 0 & 0 & 0 \end{bmatrix},$$

$$\Gamma = \begin{bmatrix} 0.00133 \\ 0.02893 \\ 0.23719 \\ 0.20959 \end{bmatrix}, \qquad \text{(A.1)}$$

$$\mathbf{H} = [1 \quad 0 \quad 0 \quad 0]$$

$$\mathbf{K} = [1.382 \quad 1.591 \quad 1.010 \quad 2.309]$$

$$\mathbf{K}_p = [-0.014 \quad -0.303 \quad -2.365 \quad -0.514 \quad -0.089]$$

$$\mathbf{L} = [0.470 \quad 0.398 \quad 0.093 \quad 0.021]^T \qquad \text{(A.2)}$$

(2) FDP System

$$\Phi = \begin{bmatrix} 1.2810 & 1 & 0 & 0 \\ -0.2461 & 0 & 1 & 0 \\ 0.0514 & 0 & 0 & 1 \\ -0.0863 & 0 & 0 & 0 \end{bmatrix},$$

$$\Gamma = \begin{bmatrix} 0.00004680 \\ 0.00101501 \\ 0.00832209 \\ 0.00735388 \end{bmatrix}, \qquad \text{(A.3)}$$

$$\mathbf{H} = [1 \quad 0 \quad 0 \quad 0]$$

$$\mathbf{K} = [92.660 \quad 86.530 \quad 78.311 \quad 63.038]$$

$$\mathbf{K}_p = [-0.169 \quad -3.687 \quad -30.387 \quad -30.913 \quad 4.985]$$

$$\mathbf{L} = [0.438 \quad -0.032 \quad 0.005 \quad -0.026]^T \qquad \text{(A.4)}$$

APPENDIX B

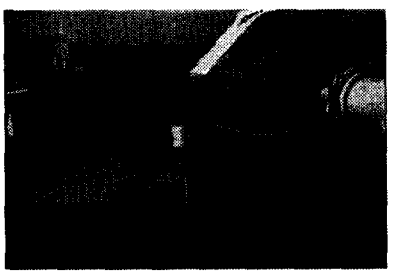

Fig. 18 Experimental system apparatus

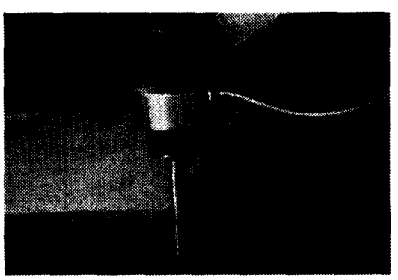

Fig. 19 Straight edge-following

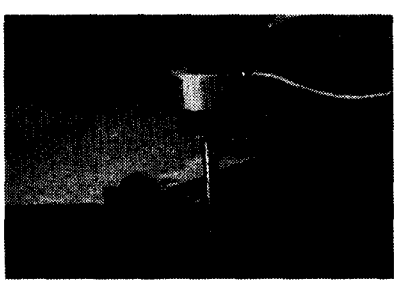

Fig. 20 Step change in contour

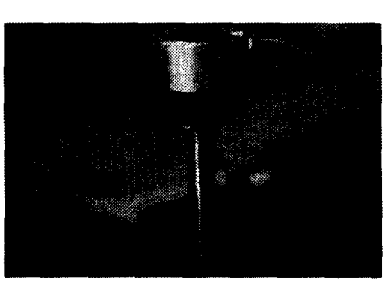

Fig. 21 Curved edge-following